Carbon dioxide snow storms during the polar night on Mars

Anthony Colaprete*, Owen B. Toon†

*NASA Ames Research Center

Moffett Field MS 245-3, Mountain View, CA

(650) 604-2918

tonyc@freeze.arc.nasa.gov

†Laboratory for Atmospheric and Space Physics

University of Colorado, Boulder, CO 80309

The Mars Orbiter Laser Altimeter (MOLA) detected clouds associated with topographic features during the polar night on Mars. While uplift generated from flow over mountains initiates clouds on both Earth and Mars, we suggest that the Martian clouds differ greatly from terrestrial mountain wave clouds. Terrestrial

wave clouds are generally compact features with sharp edges due to the relatively small particles in them. However, we find that the large mass of condensible carbon dioxide on Mars leads to clouds with snow tails that may extend many kilometers down wind from the mountain and even reach the surface. Both the observations and the simulations suggest substantial carbon dioxide snow precipitation in association with the underlying topography. This precipitation deposits CO_2, dust and water ice to the polar caps, and may lead to propagating geologic features in the Martian polar regions.

The Mars Orbiter Laser Altimeter (MOLA) used a 1.064 μm laser to measure distances from the spacecraft to the surface but it frequently detected reflections from clouds rather than the surface. In the North pole region up to 70-80% of all laser echoes on a given orbit have a cloud signature[1]. In some cases these echoes have distinct sloping edges (see Fig. 1). About half of the clouds are correlated with some sort of surface topography[1,2]. It has been suggested that, analogous with terrestrial mountain clouds, these Martian clouds contain particles too small to precipitate out and represent the sloping sides of propagating buoyancy or gravity waves[1, 2]. Using a time dependent microphysical model that incorporates CO_2 microphysics [3,4], we simulate the formation of CO_2 mountain wave clouds in a Martian polar atmosphere and compare the model results with the observations of MOLA. We find the Martian clouds contain large precipitating particles.

Mountain Waves

Orographic or mountain waves result from the flow of stratified (stable) air over surface

topography[5]. The upward motion of the air over the topography results in adiabatic cooling and thus forces buoyancy oscillations. Clouds may form within cooler regions of upward displacement. The sloping echo structures seen by MOLA could represent the tops of CO_2 clouds forming in propagating gravity waves with coherent wave fronts extending up from the surface (see Fig. 2). In this scenario perturbations in temperature induced by the vertically propagating wave lead to the formation of clouds at all altitudes wherever supersaturation is achieved[2]. However, at lower altitudes the amplitude of the propagating wave is relatively small and the resulting supersaturation is not sufficient to nucleate CO_2 cloud particles[6]. An alternate explanation for the sloping echo structures is shown in Fig. 2. The structures are still the product of mountain wave cloud formation. However, rather than clouds forming from the surface to higher altitudes along coherent wave fronts, the formation of the cloud occurs only at high altitude where the maximum cooling occurs[7,8]. Because of the high supersaturations present during nucleation, condensation occurs rapidly[4,6]. Due to the large amount of CO_2 condensing, very large CO_2 ice particles form[4,6]. As these ice particles fall they are blown in the wind forming long "snow" tails. Because the air is nearly saturated at all altitudes and the particles are so large[4,6], even in warming descending air, these particles don't evaporate entirely and can fall to the ground.

Wave Cloud Simulation

We simulated orographic waves using a microphysical cloud model that had been used previously to predict cloud microphysical characterisitcs for terrestrial wave clouds[3,4,6,7] and an analytic orographic wave model[8,9]. The initial temperature profile was determined from the vapor pressure curve for CO_2 such that for all altitudes below

30 km the CO_2 humidity relative to CO_2 ice was 98%, constant with radio occultation measurements[10] and GCM simulations[11]. In this simulation small ($r_o \sim 1$ μm) ice covered dust grains are assumed to be the nucleation sites for the CO_2 cloud particles[4,6,12].

The surface topography is modulated with time giving the appearance of a parcel of air moving at a fixed speed over the surface. The size and frequency change of the topography along with the surface wind speed will determine the properties of the wave induced[5,8]. In general, for stable stratified conditions, wide ridges (~ 10 km) with wind speeds of less than 5 m sec^{-1} provide the most favorable conditions for the formation of vertically propagating waves. Under these conditions the greatest amount of cooling occurs at levels just below the wave breaking altitude[9] and a large number of new CO_2 cloud particles form.

For cloud particles formed in the simulation, the back-scattering amplitude, described by the scattering phase function, is solved for using Mie theory. From this back-scatter amplitude the back-scatter cross section, β, of the simulated clouds can be calculated. The back-scatter cross section is defined here as the product of the average particle cross section with the back-scattering amplitude. Typical back-scatter cross sections are 100 - 300 $\mu m^2\ km^{-1}$. To compare these back-scatter cross sections with MOLA observations, the observed average back-scatter cross section was calculated using the single scatter approximation[13]. The calculated back-scatter cross sections for a MOLA pass over the northern polar region are shown in Fig. 1b. In any single cloud event, the particle back-scatter cross sections are fairly constant, with an average cross section of 200 $\mu m^2\ km^{-1}$ corresponding to a particle radius of approximately 1000 μm

(assuming 35% of the atmospheric mass at 20 km is condensed to form a cloud with an optical depth over a 400 meters path length equal to one at a wavelength of 1.064 μm). However, from one pass to another, the cross section may vary by as much as a factor of two.

Comparison with MOLA observations

The simulation presented here uses the measured topography from the MOLA pass number 226. This topography is indicated in Figure 3 by the gray shaded regions. For a 5 m sec^{-1} surface wind flowing from the left to the right a cloud forms over the first ridge at an altitude of about 18 km. Before reaching the ground the falling CO_2 ice crystals blow approximately 20 km down wind. The back-scatter cross section calculated from the simulated cloud are plotted (contours) together in Fig 3 along with the MOLA measured echo returns (filled dots). There is good agreement with both the altitude and the horizontal extent of the clouds, as well as the location of formation relative to the surface topography. The color shading of the MOLA echo data indicates the magnitude of the back-scatter cross sections calculated from the MOLA observations for the same portion of pass 226. Here too there is good agreement between the magnitude of the back-scatter cross section, as calculated from the cloud simulation, and the back-scatter cross sections derived from MOLA observations.

In many of the simulations, including the one just presented, the cloud particles fall to the ground before evaporating. The calculated integrated mass flux of CO_2 ice particles to the surface for a simulation of MOLA pass number 266 is shown in Fig. 3 (green dashed line belonging to the right vertical axis). The average size of the ice

particles that are being deposited to the surface is about 200 μm. The ice coated dust particles that these CO_2 ice crystals formed on are typically about 5 μm in diameter giving an integrated CO_2 dust to ice mass ratio of < 0.01 %. This is about 5 times lower than estimates using the Thermal Emission Spectrometer observations to model the radiative behavior of the polar caps[14]. The discrepancy occurs because of further modification of the ice crystals once on the surface[15] and by a seasonal enhancement of dust concentrations as CO_2 ice evaporates in the summer months.

Conclusions

The formation of carbon dioxide clouds requires a supersaturation of about 35%[6]. This requirement largely determines the characteristics of CO_2 cloud particles and where they will form[3,4]. The adiabatic cooling associated with orographic waves is sufficient to achieve the supersaturations required to nucleate new cloud particles. The wave-breaking altitude primarily determines the altitude of the clouds since that is where the largest amplitude waves and greatest temperature perturbations occur.

Significant amounts of CO_2 ice can be deposited to the surface during one of these snowstorms. In the simulations done here over an one-hour period as much as 0.75 grams of CO_2 snow (Fig 3) may be deposited per cm^2. The deposition of snow will be associated with the location of the wave clouds and hence the underlying topography. Snow accumulation at the tops and lee sides of ridges may explain some of the differences in surface brightness measured by TES and seen by the Mars Orbital Camera (MOC). In particular, bright crater rims, plateaus, and linear streaks running the length of ridges[14, 16] may be the result of enhanced accumulation of CO_2 and water

ices associated with the wave activity produced by these topographic features. The continued deposition of dust and retention of water ice associated with the nuclei of the CO_2 cloud particles will further modify the polar terrain by burying seasonally condensed CO_2 (down wind of the wave). Over geologic time, this process may result in a propagation of terrain, analogous to dune fields and may assist in the modulation of terraces and layering in specific regions. Being optically thick, these carbon dioxide clouds most certainly effect the radiation field during the polar night and lead to low brightness temperatures as suggested by Forget and Pollack[17] and others[18, 19, 20, 21].

While mountain wave clouds are a common occurrence on Earth, the high condensate mass on Mars make these clouds unlike their terrestrial counterparts. Terrestrial wave clouds are composed of relatively small particles (around 5 μm in size), which do not fall far and evaporate quickly[7]. The snow generated in Martian wave clouds is able to survive for a long time as it is blown downwind. The long "tail" of snow originating at altitudes in excess of 5 km can extend for 10's of kilometers down wind and deposit substantial amounts of ice to the surface. These clouds represent a subset of clouds within the polar hood. Diffuse, optically thin water clouds composed of fine particles (< 2 μm) are ubiquitous at all Martian latitudes[3, 22, 23] and additional CO_2 clouds can form if ice crystals are lifted by synoptic scale systems into slightly supersaturated regions. Regardless, because of their frequency, total mass and spatial extent, these carbon dioxide wave clouds play a critical role in both the CO_2 mass and radiation budgets of the poles.

Methods

Microphysical Cloud Model

The microphysical model includes the processes of nucleation, condensation/evaporation, and sedimentation. It is based on terrestrial models that have been used to study cirrus wave clouds, polar stratospheric clouds, and stratus clouds [7]. A contact parameter of 0.95 was used for all simulations. Transport of gases, particles and potential temperature from one altitude bin to another is allowed via sedimentation, diffusion and vertical advection. Sedimentation velocities are calculated for two regimes. A Stokes-Cunningham expression is employed for Reynolds numbers $< 10^{-2}$ and empirical interpolations are used for Reynolds numbers greater than 10^{-2}. Diffusion is handled by an eddy diffusion scheme in which the diffusion coefficients are calculated by a boundary layer turbulent mixing model. Advection is calculated using a linear wave model.

The model has 50 altitude bins each 1.0 km in thickness. The size distributions of both ice-coated dust and cloud particles are divided across 50 bins that range in size from .01 μm to 5000 μm. The ice coated dust distribution is assumed to initially have a log normal size distribution with a modal radius of $r_o = 0.1$ μm (note on top of pg. 4 you say ro is 1μm)and an integrated number concentration of 50 cm^{-3} mixed uniformly with height.

Wave Model

For a horizontal wind speed, constant in the vertical and in time, the equation for the vertical velocity perturbation, w', associated with internal gravity waves is

$$\frac{\partial^2 w'}{\partial x^2} + \frac{\partial^2 w'}{\partial z^2} + \frac{N^2}{\bar{u}^2} w' = 0$$

In this equation x and z are the horizontal and vertical distances respectively and N is the Brunt-Vaisala frequency given by

$$N = \frac{g}{T}(\Gamma_d - \Gamma)^{1/2}$$

where Γ_d and Γ are the dry and atmospheric lapse rates respectively. Typical values for N in the Martian atmosphere are between 5 x 10^{-3} and 10^{-2} s^{-1}. A solution to this equation for statically stable stationary waves forming over a ridge is

$$w(x,z) = e^{z/2H} \sum_{s=i}^{\infty} \mathrm{Re}\left(w_s \exp[i(k_s x + m_s z)]\right)$$

yielding the dispersion relation $m_s^2 = N^2/\bar{u}^2 - k_s^2$. Here k and m are the horizontal and vertical wave numbers respectively and subscript s indicates the s^{th} Fourier component. The atmospheric scale height is $H = RT/Mg$. For mechanical topographic forcing the gravity wave vertical velocity amplitude w_s can be related to the height of the topography (at the zonal wave number k_s) h_T by:

$$w_s = k_s \bar{u} h_T$$

A vertical propagating gravity wave will grow in amplitude as $p^{-1/2}$ (where p is pressure) until the waves become unstable and "break"[7]. The breaking altitude of these waves occurs at the level where the local lapse rate, the sum of that due to both the waves and the mean state, first exceeds the dry adiabatic lapse rate[8]. Above the breaking altitude the wave dissipates through turbulence.

Back-scatter Cross Sections

The back-scatter cross section is a measure of the ability for a particle to scatter light

backward and depends on the size, or cross section, of the scattering particle and its shape. For a single scatter approximation the back-scatter cross section, β, may be written

$$\beta = 4\pi \frac{P_r}{P_t} \frac{A_t}{A_r} \frac{l^2}{T}$$

where P_t and P_r are the laser power transmitted and received respectively, A_t is the area of transmitted laser footprint at the cloud tops, A_r is the collecting area of the receiver, l is the range distance to the cloud tops, and T is the attenuation of the laser by the atmosphere. The atmospheric attenuation is defined as $T = \alpha e^{-2\tau}$ where α is the surface albedo and τ is the atmospheric total optical depth.

References and Notes

1. Zuber, M. T. et al.,Observations of the north polar region of Mars from the Mars Orbiter Laser Altimeter, *Science* **282**, 2053, (1998).
2. Pettengill, G. H. and P. G. Ford, Winter clouds over the north Martian polar cap, *Geophys. Res. Lett.* **27**, 609 (2000).
3. Colaprete A., O. B. Toon and J. A. Magalhães, Cloud formation under Mars Pathfinder conditions, *J. Geophys. Res.* **104**, 9043 (1999).
4. Colaprete, A. and O. B. Toon, Carbon dioxide clouds at high altitude in the tropics and in an early dense Martian atmosphere, *Icarus*, submitted (2001).
5. J. R. Holton, *Dynamic Meteorology*, Academic Press (1992).
6. Glandorf, D., A. Colaprete, O. B. Toon, and M. Tolbert, CO_2 snow on Mars: experimental constraints, *Icarus*, submitted (2001).
7. Jensen et al., Ice nucleation processes in upper tropospheric wave-clouds observed during SUCCESS, *Geophys. Res. Lett.* **25**, 1363 (1998).
8. R. S. Lindzen, Turbulence and stress owing to gravity wave tidal breakdown, *J. Geophys. Res.* **86**, 9707 (1981).
9. J. R. Barnes, Possible effects of breaking gravity waves on the circulation of the middle atmosphere of Mars, *J. Geophys. Res.* **95**, 1401 (1990).
10. Hinson, D. P., F. M. Flasar, R. A. Simpson, J. D. Twicken and G. L. Tyler, Initial results from radio occultation measurements with Mars Global Surveyor, *J. Geophys. Res.* **104**, 26997 (1999).
11. Haberle, R. M., H. C. Houben, R. Hertenstein, and T. Herdtle, A boundary-layer model for Mars: Comparison with Viking Lander and entry data, *J. Geophys. Res.* **98**, 3093 (1993).
12. Pearl, J. C., M. D. Smith, B. J. Conrath, J. C. Bandfield, and P. R. Christensen, Mars

Global Surveyor TES results: observations of water ice clouds, *American Astronomical Society*, DPS #31, #76.08, 1999.
13. Stephens, G. L., *Remote sensing of the lower atmosphere*, Oxford University Press, 1994.
14. B. H. Hansen, Control of the radiative behavior of the Martian polar caps by surface CO_2 ice: evidence from the Mars Global Surveyor measurements, *J. Geophys. Res.* **104**, 16,471 (1999).
15. Clark, R. N., F. P. Fanale, and A. P. Zent, Frost grain size metamorphism: implications for remote sensing of planetary surfaces, *Icarus* **56**, 233 (1983).
16. H. H. Kieffer. T. Titus, K. Mullins, Early TES observations of the south polar region, Lunar and Planetary Science XXIX, Abstract 1481, Lunar and Planetary Institute, Houston (CD-ROM) (1998).
17. F. Forget, and J. B. Pollack, Thermal infrared observations of the condensing Martian polar caps: CO_2 ice temperatures and radiative budget, *J. Geophys. Res.* **101**, 16,865 (1996).
18. D. A. Paige, and A. P. Ingersoll, Annual heat balance of Martian polar caps: Viking observations, *Science* **228**, 1160 (1985).
19. F. Forget, F. Hourdin, and O. Talagrand, CO_2 snowfall on Mars: simulated with a general circulation model, *Icarus* **131**, 302 (1997).
20. H. H. Kieffer, et al., Infrared thermal mapping of the Martian surface and atmosphere: first results, *Science* **193**, 780 (1976).
21. G. E. Hunt, On the infrared radiative properties of CO_2 ice clouds: application to Mars, *Geophys. Res. Lett.* **7**, 481 (1980).
22. R. Kahn, 1990, Ice haze, snow, and the Mars water cycle, *J. Geophys. Res.* ***95***, 14,677 (1990).
23. R. T. Clancy et al., Water vapor saturation at low altitudes around Mars aphelion: a key to Mars climate?, *Icarus **122***, 36 (1996).

Acknowledgements
Funding for this work came from NASA's Planetary Atmosphere's grant NAG5-6900 and from NASA's Astrobiology Program, NCC2-5300 and NCC2-1052.

Figure 1 Echo returns from MOLA pass number 232 (a) and the average back-scatter cross section calculated from laser energy return at 1.067 μm for the same MOLA pass (b). The long sloping features that extend from the surface to nearly 6 km in altitude (part a) are the subject of the discussion here and are believed to be carbon dioxide "snow tails".

Figure 2. A cartoon showing the stream lines that would be produced from a stationary, altitude independent flow over a single ridge. Also shown in this figure are the regions of possible cloud formation (indicated by the shaded regions). As the waves propagate upward their amplitude will increases leading to greater cooling and thus higher supersaturations (S) at higher altitudes. It is in these regions that CO_2 clouds will form. Precipitation from these clouds will fall downward, blowing down wind (indicated by the speckled region). (This fig looks odd, it seems to have a big black block for the snow. Maybe it is just not read right by my computer.)

Figure 3. The simulated average back-scatter cross section at 1.067 μm for a 5 m sec^{-1} surface flow over the topography as measured by MOLA during pass number 226. The shaded region represents the measured topography. MOLA echoes for the same pass are shown as solid colored dots. The color of each dot represents the back-scatter cross section (color scale at the top of the figure) derived from MOLA laser energy data as described in the text. Contours show the back-scatter cross sections calculated for the simulation. The contour magnitude is designated by the same color as the MOLA echoes (dots). Also shown (green dashed line with right axis) is the calculated mass flux of CO_2 ice particles to the surface for a segment of MOLA pass 226 between 0 and 100 km. For the simulation presented here in an one hour snow storm approximately 0.75 g cm^{-2} of CO_2 snow may be deposited to the surface.

Colaprete_fig1

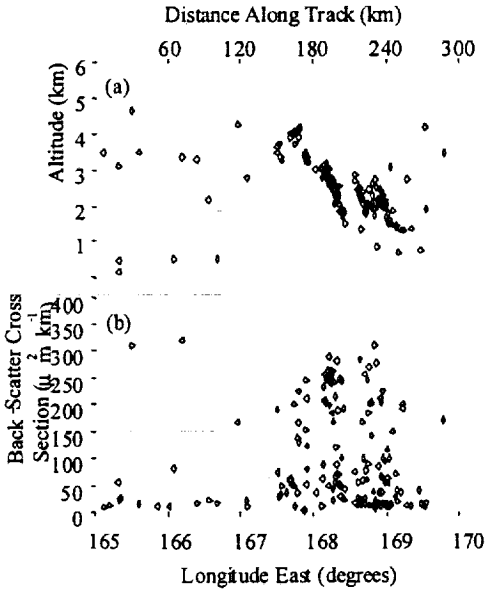

Colaprete_fig2

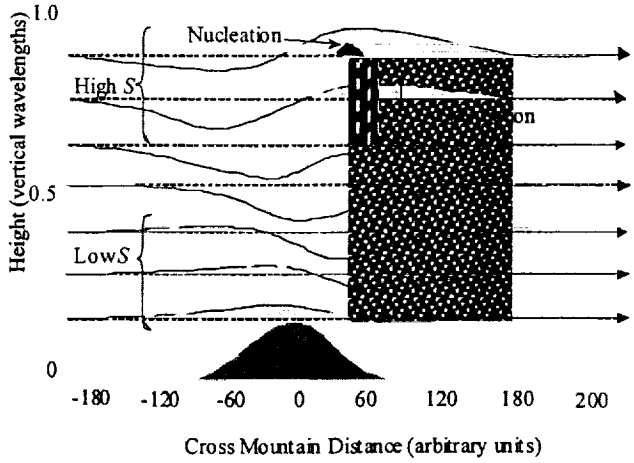

Colaprete_fig3